

Importance of a second entrance in a test cell

Oana DUMITRESCU^{*1}, George Bogdan GHERMAN¹, Ionut PORUMBEL¹

*Corresponding author

¹COMOTI – National Research and Development Institute for Gas Turbines,
B-dul Iuliu Maniu 220, Bucharest 061126, Romania
oana.dumitrescu@comoti.ro*, bogdan.gherman@comoti.ro,
ionut.porumbel@comoti.ro

DOI: 10.13111/2066-8201.2018.10.1.7

Received: 20 November 2017/ Accepted: 17 January 2018/ Published: March 2018

Copyright © 2018. Published by INCAS. This is an “open access” article under the CC BY-NC-ND license (<http://creativecommons.org/licenses/by-nc-nd/4.0/>)

Aerospace Europe CEAS 2017 Conference,

16th-20th October 2017, Palace of the Parliament, Bucharest, Romania

Technical session Propulsion II

Abstract: *The present paper studies the influence of a secondary intake and its effect on the jet stability. Three configurations have been analyzed: one with the secondary intake closed, the second having a convergent nozzle after the augmentor tube and the third case using a perforated augmentor tube. The secondary intake is used to supply air for cooling the exhaust system. Numerical simulation was realized using the *k-ε* model, which is the most used CFD turbulence model, especially for turbulent flow conditions. The results obtained showed that secondary intake influences the jet stability, because of the pressure differences from the two zones. To resolve this closing the secondary intake is the best option available.*

Key Words: *CFD, secondary intake, test cell.*

1. INTRODUCTION

The main purpose of an experiment test cell is to provide a controlled environment for engine testing; characteristics of the environment are very important for the aerodynamic performances, operation stability of the engine and acoustic control [1].

The problems that can influence the operation stability of an engine are given by the design of the test cell inlet, exhaust systems and to the cell bypass ratio [1]. Cell bypass ratio is the ratio of the airflow bypassing between the engine and the internal walls of the cell, and cools the engine [9].

Test cell systems must follow some criteria: must reduce engine noise to a reasonable level, must ensure an internal environment that provides a clean air flowing to the engine, also a minimum pressure loss. Under most environmental conditions, a test cell configuration should not allow recirculation of engine exhaust gases from the cell exhaust stack into the cell inlet. It should also prevent reinjection of engine exhaust gases at the rear of the engine back into the engine inlet [3].

Air intake, that is one of the most important parts of the test cell, is either vertical or horizontal. With a horizontal intake the flow is directed to the engine without having to turn through 90°. Side walls are build in front test chamber so that the air will not be influenced by the cross winds. It's important to have good quality airflow, this is crucial for the

measurements of the engine performances. Vertical intakes because of using flow splitters and straightness reduce substantially the adverse effects [8]. On the secondary intake is not necessary that the aerodynamically clean, noise attenuation is just as important as in the case of primary intake. An important aim of the augmentor is to take the hot gases and direct them uniformly towards the exhaust stake [2]. At the secondary intake, the air is mixed with the exhaust gases leading to a decrease of the hot gases temperature. The most important condition of the test cell configuration is to not allow the recirculation of the exhaust gases from the exhaust stack into the inlet cell [3].

In 1989, E. E. Cooper and C. A. Kodres were testing a U.S. Navy standard test cell experimentally to determine the aerodynamic and experimental characteristics. They have measured the pressure and temperature in the cell while testing different engines at different power settings. Setting the engine power from idle to military increases total test cell airflow, but when afterburner is initiated remains constant.

Another important aspect observed was the slight upward and sideways skewing of the velocity and temperature profiles in the augmentor tube [7].

Air flow stability and engine measurements are compromised if the depression in the test cell is not limited. Jacques [4] states that a difference between the ambient and the chamber static pressure up to 150 mmH₂O (1470 Pa) is unlikely to be a problem for the engine work conditions.

In this paper three different situations were analyzed: one with the secondary intake closed, the second having a convergent augmentor and the third case using a perforated augmentor. The objectives of this study are to obtain a uniform secondary inlet flow along with the velocity reduction at the primary inlet, because a non-uniformity of the secondary inlet flow would affect the shape of the jet leaving the engine.

2. PROBLEM SETUP

Geometry definition

The study performed in this paper is made using the commercial software ANSYS CFX. The test cell consists of a primary intake, the main test chamber, a secondary intake, an augmentor tube and the exhaust stack, presented in Fig. 1. For both the primary intake and the secondary intake acoustic baffles for noise reduction, are used. For the primary intake turning vanes are used to provide a uniform air flow for the main chamber.

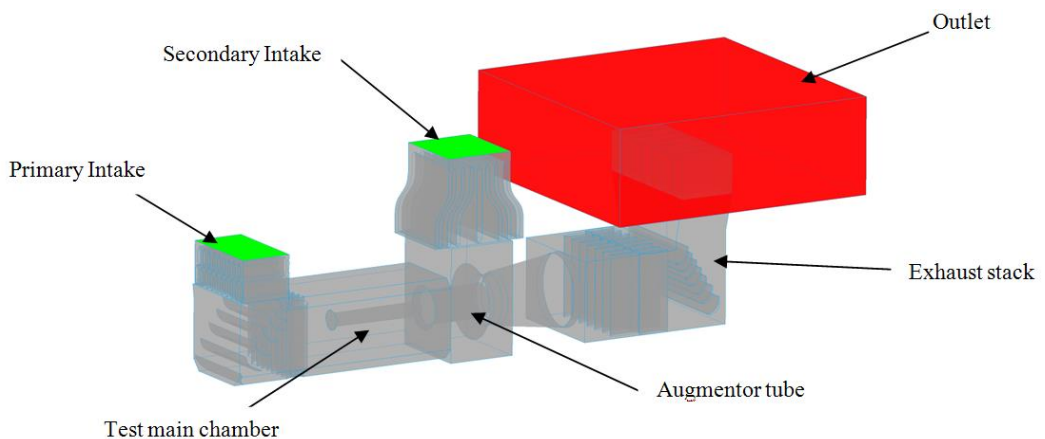


Fig. 1 – Geometry of the test cell

The principal features of the test cell are presented in Table 1.

Table 1 – Geometrical parameters of the test cell

Domain	Parameter – System of units	Dimensions
Test cell length	[mm]	27315
Test cell width	[mm]	5800
Primary intake	Length [mm]	2615
	Width [mm]	4780
Secondary intake	Length [mm]	3500
	Width [mm]	4000
Outlet	Length [mm]	14000
	Width [mm]	14020
Engine length	[mm]	5000
Distance between engine and augmentor tube	[mm]	500

Mesh

The grid used in this study is made with ANSYS ICEM CFD, and the grid generated for this test cell is unstructured, due to the complex geometry. For all the cases the discretization is made using tetrahedral elements, Fig. 2. Mesh details are given in Table 2.

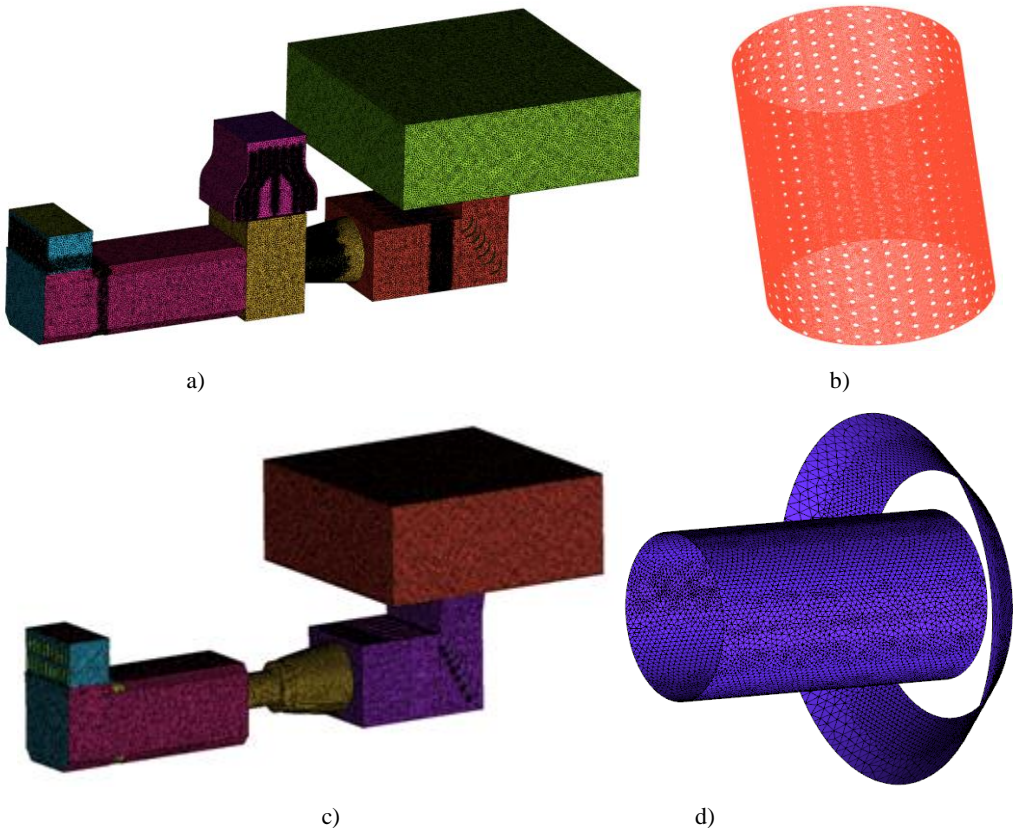


Fig. 2 – a) Grid generated for all the three cases; b) perforated augmentor tube; c) secondary intake closed, d) convergent nozzle

Table 2 – Mesh details

Case	Number of nodes	Number of elements
secondary intake closed	1.74 million	10.37 million
perforated augmentor tube	4.12 million	24.5 million
convergent nozzle	3.66 million	21.66 million

The fluid used for this case is ideal air. Reference pressure is 1 bar, and the temperature is 288.15 K (15°C). Boundary conditions used for this numerical simulation are presented in Table 2.

Table 3 – Boundary conditions

Domain		System of units	Value
Mass flow at engine inlet		[kg/s]	64
Mass flow at engine exhaust		[kg/s]	68
Total temperature at engine exhaust		[K]	983
Outlet	Opening pressure and direction	[bar]	0
	Opening temperature	[K]	300.15

The engine used in this case is Tumansky R11 – F300, also the calculations are done for the case with afterburner.

Turbulence model

For these simulations a k- ε turbulence model has been used. This turbulence model is one of the most used CFD turbulence model, especially for turbulent flow conditions. It's very popular in industrial applications, due to the good convergence rate and because it does not require very large computing resources [6].

The model is based on two equations describing the turbulence. The first one allows the determination of turbulent kinetic energy and the second the dissipation rate of turbulent kinetic energy. For the turbulent kinetic energy – k [5]:

$$\frac{\partial(\rho k)}{\partial t} + \frac{\partial(\rho k u_i)}{\partial x_i} = \frac{\partial}{\partial x_j} \left[\left(\mu + \frac{\mu_t}{\sigma_k} \right) \frac{\partial k}{\partial x_j} \right] + 2\mu_t E_{ij} E_{ij} - \rho \varepsilon \tag{1}$$

For dissipation – ε [5]:

$$\frac{\partial(\rho \varepsilon)}{\partial t} + \frac{\partial(\rho \varepsilon u_i)}{\partial x_i} = \frac{\partial}{\partial x_j} \left[\left(\mu + \frac{\mu_t}{\sigma_\varepsilon} \right) \frac{\partial \varepsilon}{\partial x_j} \right] + C_{1\varepsilon} \frac{\varepsilon}{k} 2\mu_t E_{ij} E_{ij} - C_{2\varepsilon} \rho \frac{\varepsilon^2}{k} \tag{2}$$

Where the eddy viscosity is defined as follow: $\mu_t = \rho C_\mu \frac{k^2}{\varepsilon}$

3. RESULTS

Due to the steady RANS calculation, accuracy of the calculation is limited by the method used, but considering the resources available accuracy is sufficient to attain the study. The quantity of mass flow rate that enters on the two inlets is different. Using Ansys CFX a value of 102.8 kg/s for the primary intake and 19.7 kg/s for secondary intake, have been obtained. Fig. 3 shows velocity variation in the X direction. As can be seen in the first case Fig. 3.a), the secondary intake influences the shape of the jet, which becomes instable. Secondary

intake provides an increase in velocity, as well as shortening the length of the jet. Also in the case of Fig. 4.a) it can be noticed how the fluid spreads to the inlet area, as well as the occurrence of shock waves upon contact with the tube interface. In case Fig. 3.c) an improvement of the flow field, caused by a decrease in pressure difference, given by the convergent augmentor, is observed.

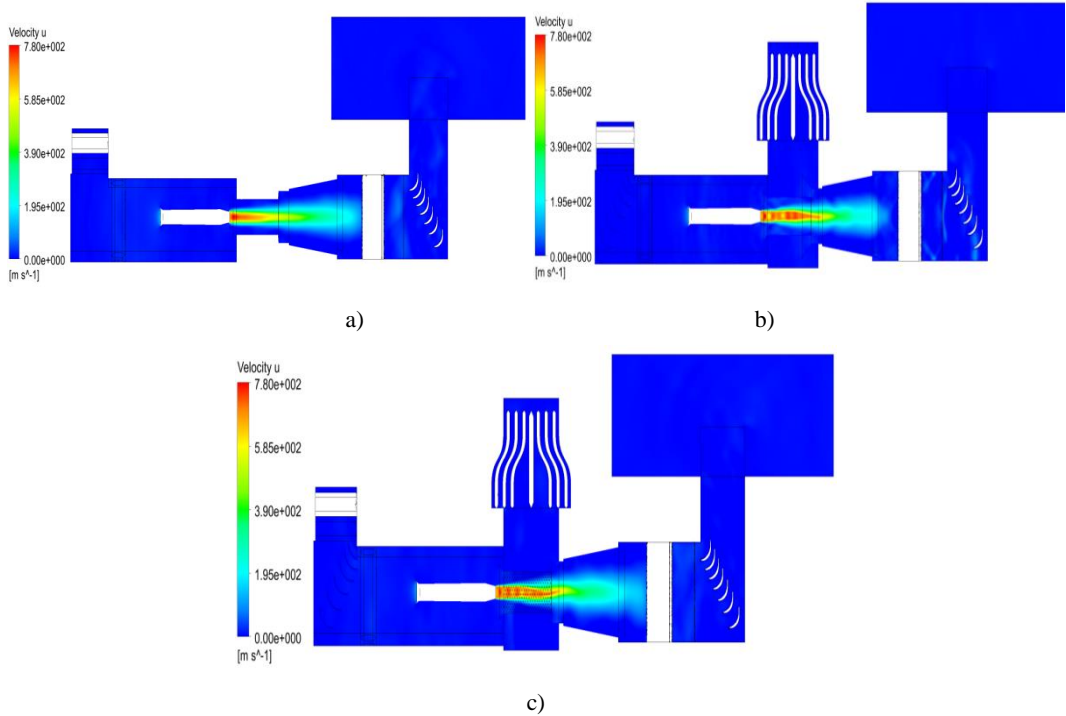


Fig. 3 – Velocity variation in the X direction, XZ plan

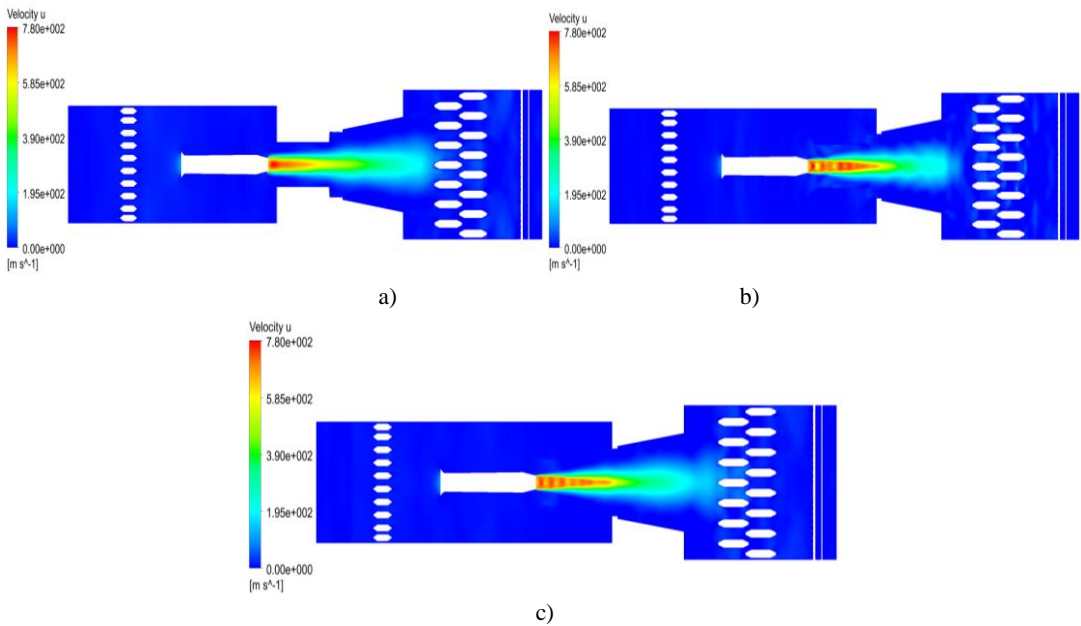


Fig. 4 – Velocity variation in the X direction, XY plan

The secondary fluid inlet does not only influence the velocity, but also the temperature (Fig. 5).

The output temperature is much higher when the second input is open. This also influences the length and shape of the jet.

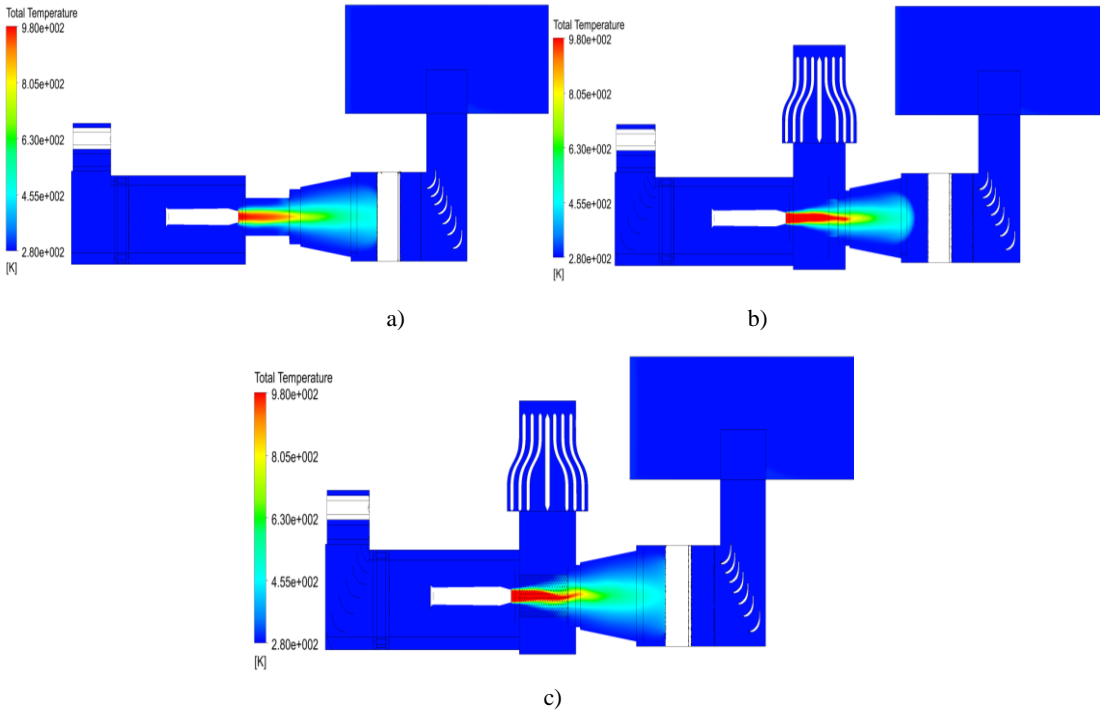


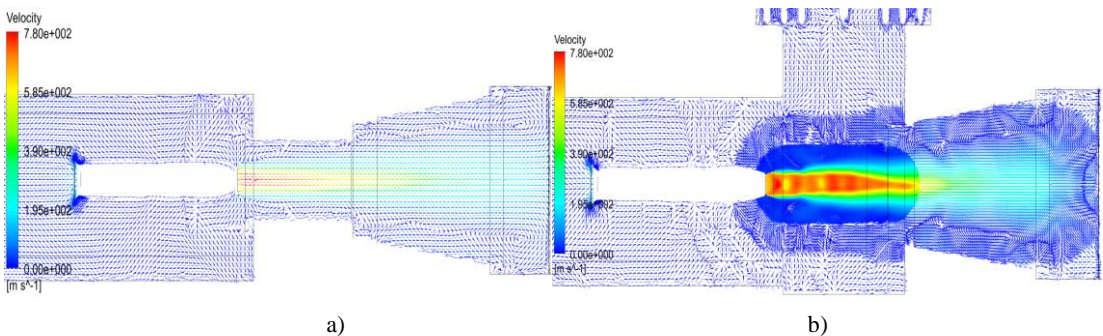
Fig. 5 – Total temperature variation, XZ plan

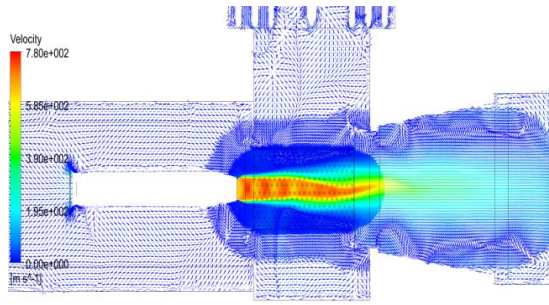
Also, Fig. 6 shows the vector field at the engine exhaust area. These show how the fluid enters the augmentor tube.

As can be seen in Fig. 6.a) and Fig. 6.c), there are recirculation areas in the proximity of the engine exit.

With the help of an isosurface, the shape of the jet is illustrated in Fig. 7. It can be seen that in the case of first geometry the length of the jet is shorter, compared to the other two cases, also it's stability.

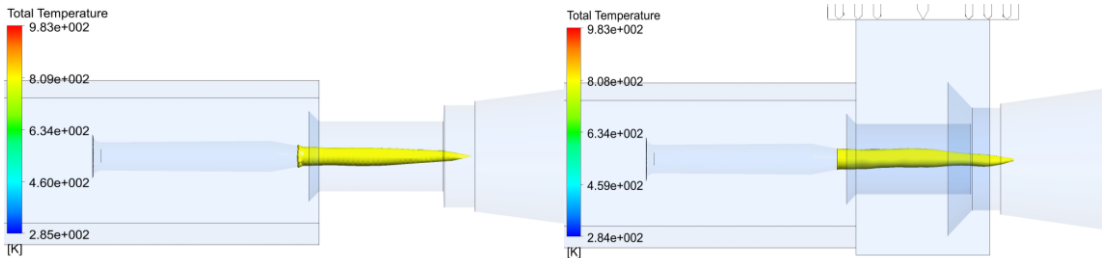
For the other two cases, near the exit from the augmentor tube, appears a variation of its shape produced by the differences in pressure on the upper and lower zone of the tube. In the case of the perforated augmentor tube, instability is more pronounced.





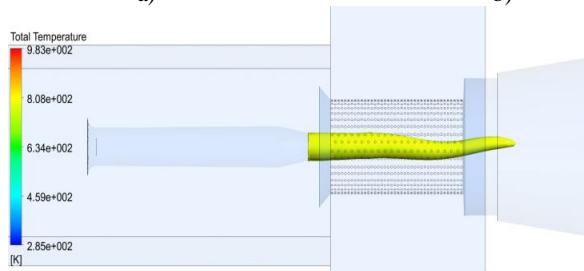
c)

Fig. 6 – Vector field after engine exit



a)

b)



c)

Fig. 7 – Isosurface corresponding to engine jet

For a better understanding of the jet instability, where considered three lines of measurement at engine exhaust: top, center and bottom. How they were positioned is illustrated in Fig. 8. Fig. 9 shows a comparison of how the velocity varies in those three critical areas. The highest value is the area in the centre of the nozzle, this applies in all cases. The velocity exceeds 800 m/s, if the secondary intake Fig. 11.a) - is open and over 700 m/s in Fig. 11.b).

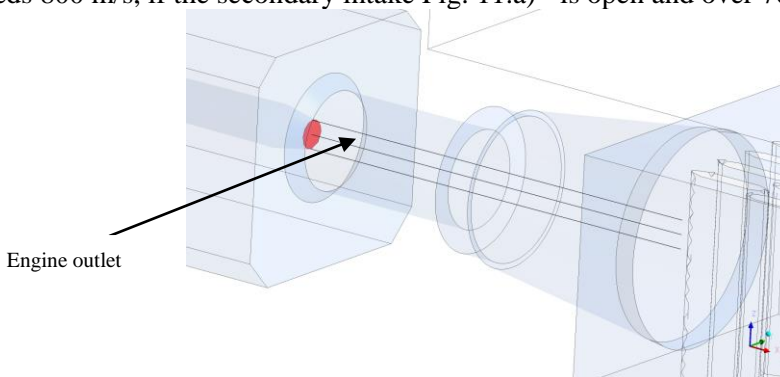


Fig. 8 – Measurement lines used to determine velocity

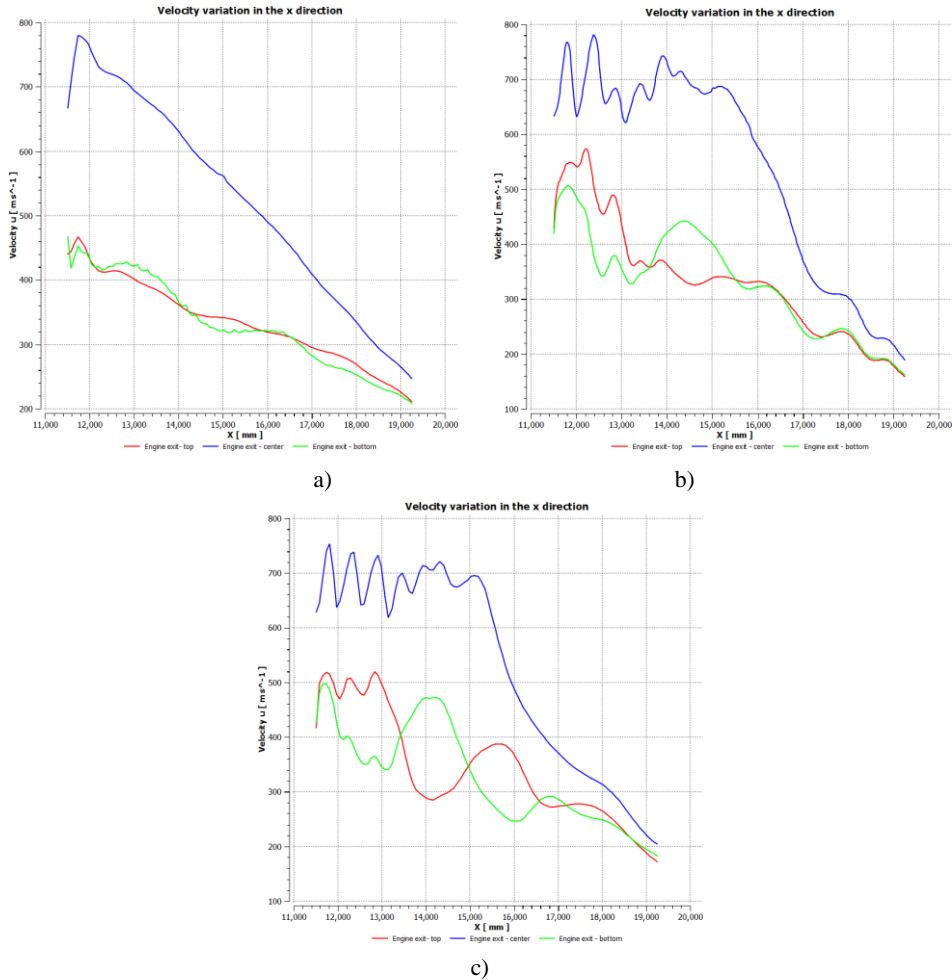
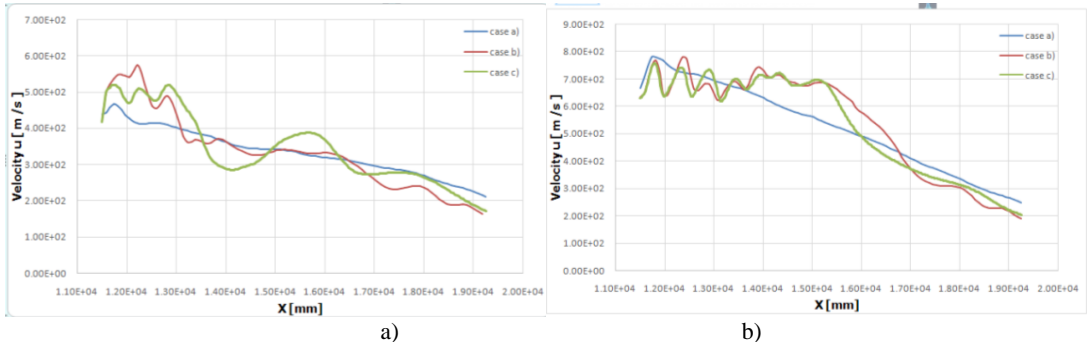
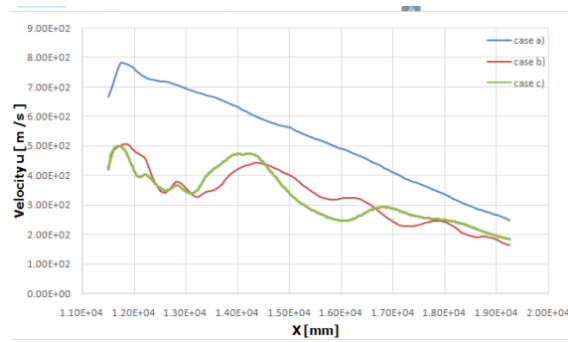


Fig. 9 – Velocity distribution after engine exit: case a), case b), case c)

In Fig. 10 are presented three charts corresponding to the three types of cases studied. In all situations it's a big difference between the values obtained in the case in which the secondary intake is closed, comparative with the other two. Also on the top and bottom the values are different, this is due the pressure difference caused by the different volume on the upper and lower zone of augmentor tube. A major dissimilarity compared with the case a) appears near the exit from the tube, there is a difference about 150K. In Fig. 10.c) can be seen that a difference about 250K.

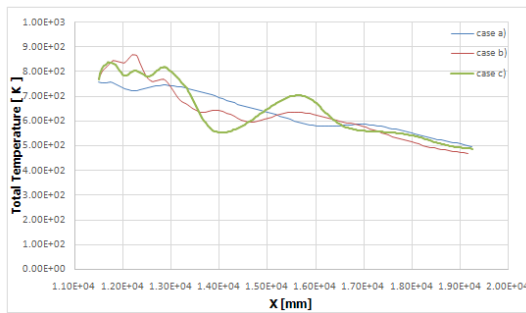




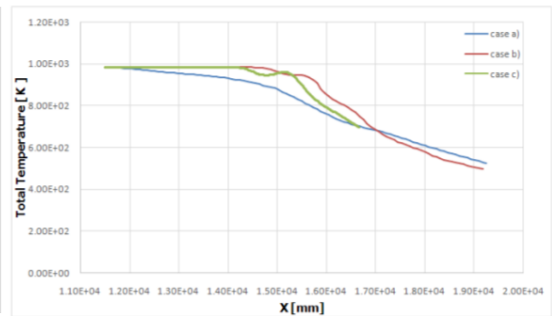
c)

Fig. 10 – Velocity distribution after engine exit: a) top, b) center, c) bottom

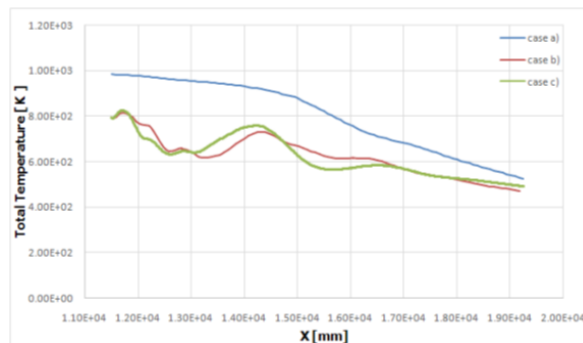
Also in the case of total temperature, the differences are still applying, Fig. 11.



a)



b)



c)

Fig. 11 – Total temperature distribution: a) top, b) center, c) bottom

4. CONCLUSIONS

This paper presents a study regarding the influence of a secondary intake on the jet stability. Three configurations have been studied: one with the secondary intake closed, the second having a convergent nozzle after the augmentor tube and the third case using a perforated augmentor tube. Where analyzed the total temperature and velocity fields in X direction, this captures have allowed us to better understand how the jet behaves in the cases studied. The results obtained showed that secondary intake influences the jet stability, and to resolve this closing the secondary intake is the best option available.

REFERENCES

- [1] * * * *Design Considerations for Enclosed Turbofan/Turbojet Engine Test Cells*, SAE International, February 20, 2015
- [2] G. L. B. Ramos, *Study of a Test Cell for Commercial Jet Engines*, Master of Science Degree in Mechanical Engineering, Técnico Lisboa, July 2015.
- [3] J. J. Ballough, *Correlation, Operation, Design, and Modification of Turbofan/Jet Engine Test Cells*, U.S. Department of Transportation, Federal Aviation Administration, 02 December, 2012.
- [4] R. Jacques, *Operation and performance measurement on engines in sea level test facilities*, AGARD Lecture Series No.132, Mar. 1984.
- [5] H. K. Versteeg, W. Malalasekera, *An introduction to Computational Fluid Dynamics: The Finite Volume Method*, Pearson Education, 2007.
- [6] D. C. Wilcox, *Turbulence Modeling for CFD*, Second edition, Anaheim: DCW Industries, pp. 174, 1998.
- [7] E. E. Cooper, C. A. Kodres, *Experimental Examination of the Aerothermal Performance of a Gas Turbine Engine Test Facility*, Gas Turbine and Aeroengine Congress and Exposition, Toronto, Ontario, Canada, June 4-8, 1989.
- [8] A. Al-Shaikh, *An Experimental and Numerical Investigation of the Effect of Aero Gas Turbine Test Facility Aspect Ratio on Thrust Measurement*, PhD Thesis, Cranfield University, August 2011.
- [9] H. W. Hua, M. Jermy, H. Dumbleton, Formation of Sink Vortices in a Jet Engine Test Cell, *Engineering Letters*, **16** (3), pp. 406-411, 2008.